Keto-coumarin scaffold for photoinitiators for 3D printing and photocomposites

Mira Abdallah, Frederic Dumur, Akram Hijazi, Giacomo Rodeghiero, Andrea Gualandi, Pier Giorgio Cozzi, Jacques Lalevee

AUTHOR QUERY FORM

Dear Author,
During the preparation of your manuscript for publication, the questions listed below have arisen. Please attend to these matters and return this form with your proof.
Many thanks for your assistance.

Query References	Query	Remarks
Q1	Please confirm that given names (blue) and surnames/family names (vermilion) have been identified and spelled correctly.	
Q2	Please check and confirm that the corresponding details have been set correctly.	
Q3	Please check if link to ORCID is correct.	
Q4	Please provide missing department names for the affiliations, if any.	
Q5	Please check and confirm that the affiliations of the authors have been set correctly.	
Q6	Please provide the “name of the publisher” for reference 11.	
Q7	The supplied figure 7 is in Low resolution. Kindly provide us the better version. Please refer to http://media.wiley.com/assets/7323/92/electronic_artwork_guidelines.pdf for the guidelines on how to produce good figures.	
Q8	Please confirm whether the color figures should be reproduced in color or Black and white in the print version. If the color figures must be reproduced in color in print version, please fill the color charge form immediately and return to the Production Editor. Or else, the color figures for your article will appear in color in the online version only.	

SPi	Journal Code	Article ID	Dispatch: 05-FEB-20	CE:
	POLA	29633	No. of Pages: 15	ME:

Received: 19 December 2019 | Revised: 26 January 2020 | Accepted: 30 January 2020

DOI: 10.1002/pol.20190290

ORIGINAL ARTICLE

JOURNAL OF POLYMER SCIENCE WILEY

Keto-coumarin scaffold for photoinitiators for 3D printing and photocomposites

Mira Abdallah[1,2,3] | Frédéric Dumur[4] | Akram Hijazi[3] | Giacomo Rodeghiero[5,6] | Andrea Gualandi[5] | Pier G. Cozzi[5] | Jacques Lalevée[1,2]

[1]IS2M UMR 7361, CNRS, Université de Haute-Alsace, Mulhouse, France

[2]Université de Strasbourg, Strasbourg, France

[3]EDST, Université Libanaise, Campus Hariri, Beyrouth, Lebanon

[4]ICR UMR 7273, CNRS, Aix Marseille University, Marseille, France

[5]Dipartimento di Chimica "G. Ciamician", Alma Mater Studiorum, Università di Bologna, Bologna, Italy

[6]Cyanagen Srl, Bologna, Italy

Correspondence
Pier G. Cozzi, Dipartimento di Chimica "G. Ciamician," Alma Mater Studiorum, Università di Bologna, Via Selmi2, 40126 Bologna, Italy.
E-mail: jacques.lalevee@uha.fr

Jacques Lalevée, IS2M UMR 7361, CNRS, Université de Haute-Alsace, F-68100 Mulhouse, France.
E-mail: piergiorgio.cozzi@unibo.it

Abstract

The purposes of this paper are moving toward (a) the development of a new series of photoinitiators (PIs) which are based on the keto-coumarin (KC) core, (b) the introduction of light-emitting diodes (LEDs) as inexpensive and safe sources of irradiation, (c) the study of the photochemical mechanisms through which the new PIs react using different techniques such as Fourier transform infrared, UV–visible or fluorescence spectroscopy, and so on, (d) the use of such compounds (presenting good reactivity and excellent photopolymerization initiating abilities) for two specific and high added value applications: 3D printing (@405 nm) and preparation of thick glass fiber photocomposites with excellent depth of cure, and finally (e) the comparison of the performance of these KC derivatives versus other synthesized coumarin derivatives. In this study, six well-designed KC derivatives (**KC-C**, **KC-D**, **KC-E**, **KC-F**, **KC-G**, and **KC-H**) are examined as high-performance visible-light PIs for the cationic polymerization of epoxides as well as the free-radical polymerization of acrylates upon irradiation with LED@405 nm. Excellent polymerization rates are obtained using two different approaches: a photooxidation process in combination with an iodonium (Iod) salt and a photoreduction process when associated with an amine (*N*-phenylglycine or ethyl 4-(dimethylamino)benzoate). High final reactive conversions were obtained. A full picture of the involved photochemical mechanisms is provided.

KEYWORDS

keto-coumarin, light-emitting diode, photocomposite, photoinitiator, photopolymerization, 3D printing resin

1 | INTRODUCTION

Keto-coumarins (KCs) are characterized by interesting photophysical properties among them are: (a) a very high and efficient singlet-triplet intersystem crossing quantum yield which makes them a potential important class of triplet sensitizer,[1,2] (b) a rather low singlet-triplet energy gap, (c) high extinction coefficients in the near UV or even visible light, and (d) long lifetime of the triplet excited state ensuring potential quenching processes. KC can be considered as an important member of coumarin dyes. In their chemical structure, a carbonyl group is directly bonded to 3-position of the coumarin core. The photophysical and photochemical properties of KCs were largely investigated.[3,4] For example, the study of the photophysical properties of KCs in different

solvents and alcohol: water binary mixture and solid state has been accomplished using steady-state, fluorescence spectroscopy and other techniques.[5] Williams and co-authors have studied different 3-KCs with alkoxy or dialkylamino substituents in the 7-position as photoinitiators (PIs). Electron-transfer quantum yields to initiate radical polymerization were calculated for different combinations based on KC/activators or co-initiators such as amines, acetic acid, and alkoxypyridinium salts in order to show that photoinitiation efficiency requires the choice of a specific activator to use with specific KC structures. Some chemical mechanisms were proposed for the generation of radicals.[6] The use of KCs to initiate free-radical photopolymerization (FRP) of multifunctional acrylate monomers under visible light in multicomponent photoinitiating systems (PISs) is also well-established (e.g., KC/1,3,5-triazine derivative/aliphatic thiol).[7–12] Other coumarin-based PIs were recently reported.[13–15]

The present paper relates to the development of a specific set of KC derivatives (Figure 1) which can be used upon near UV or visible light-emitting diodes (LEDs) thanks to their remarkable absorption in the 350–500 nm. KCs will be combined with *bis*(4-*tert*-butylphenyl)iodonium hexafluorophosphate (Iod) or *N*-phenylglycine (NPG) or ethyl 4-(dimethylamino)benzoate (EDB) as co-initiators to form two-component PISs in order to generate the initiating species (radicals or cations) that are able to trigger the photopolymerization reaction. KCs will be also incorporated into three-component (KC/Iod/NPG) PISs. LED@405 nm was chosen as a very cheap and safe irradiation source for both FRP and cationic polymerization (CP) processes; also representative of 3D printing experiments.

The purpose of the different substituents in KCs is to study the effect of such substituents on the light absorption properties, the photochemical mechanisms, the redox properties, and therefore the photopolymerization processes. The study of the photophysical and photochemical properties of KC derivatives has been provided as well as photochemical mechanisms. The comparison between the performance of the KC derivatives and two new synthesized coumarin derivatives (Coum-A1 and Coum-B1) is also supplied. The structure/reactivity/efficiency relationships will be discussed in details based on different techniques such as UV–visible spectroscopy, fluorimetry, cyclic voltammetry, and electron spin resonance (ESR). KCs are also shown exhibiting properties for 3D printing technologies but also for the manufacture of thick glass fibers/acrylate photocomposites using near-UV conveyor.

2 | EXPERIMENTAL PART

2.1 | Synthesis of KC Derivatives Studied in this Work

The full procedure for the synthesis of Coumarins and KCs (Figure 1) is provided below in Section 3.1.

2.2 | Commercial Chemical Compounds

All commercial chemical compounds were selected with highest purity available and used as received; they are presented in Scheme 1. *Bis*(4-*tert*-butylphenyl)iodonium hexafluorophosphate (Iod or SpeedCure 938) was obtained from Lambson Ltd (UK). *N*-Phenylglycine (NPG) and ethyl 4-(dimethylamino)benzoate (EDB) were obtained from Sigma Aldrich. (3,4-Epoxycyclohexane) methyl 3,4-epoxycyclohexylcarboxylate (EPOX; Uvacure 1500) and trimethylolpropane triacrylate (TMPTA) were obtained from Allnex. TMPTA and EPOX were selected as benchmarked monomers for radical polymerization and CP, respectively.

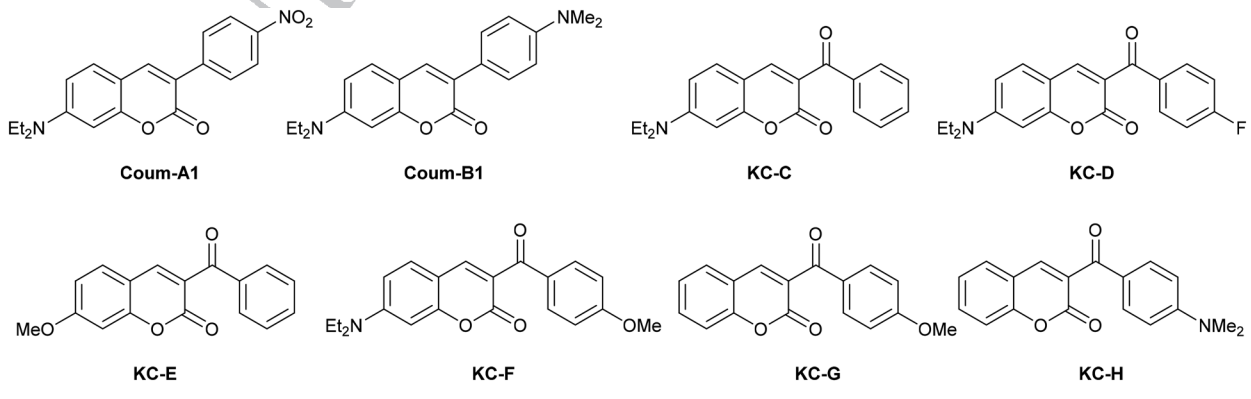

FIGURE 1 Chemical structures of the coumarins and keto-coumarins investigated in this work

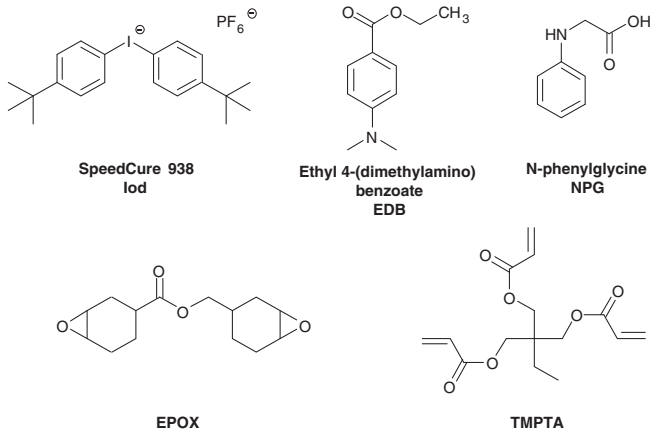

SCHEME 1 Other chemical compounds used in this work

2.3 | Light Irradiation Sources

The following LEDs, (a) LED@375 nm; incident light intensity at the sample surface: $I_0 = 40$ mW cm^{-2} and (b) LED@405 nm ($I_0 = 110$ mW cm^{-2}), were used as light irradiation sources.

2.4 | CP and FRP followed by real-time Fourier transform infrared

In this research, the two-component PISs used for FRP and/or CP are mainly based on KC/Iod salt (or NPG or EDB) (0.2%/1% w/w) couples. Otherwise, KC/Iod salt/NPG (0.2%/1%/1% w/w) combinations are used as three-component PISs for FRP. The weight percent of the different chemical compounds of the PIS is calculated according to the monomer content (w/w). BaF_2 pellet is used for the CP of EPOX which is realized under air; the photosensitive thin samples (thickness ~25 μm) were deposed on this pellet, while propylene films are used for the FRP of TMTPA thin samples which is done in laminate. The photosensitive formulations are sandwiched between two propylene films in order to reduce O_2 inhibition. For thin samples, the evolution of the epoxy group content of EPOX and the double bond content of acrylate functions were continuously followed by real-time Fourier transform infrared (FTIR) spectroscopy (JASCO FTIR 4100) at about 790 and 1,630 cm^{-1}, respectively. Otherwise, a mold of ~7 mm diameter and 1.4 mm of thickness is used for the FRP of TMPTA thick samples and the characteristic peak of acrylate was followed in the near-infrared range at ~6,160 cm^{-1}. The procedure used to monitor the photopolymerization profiles has been already described in detail.[16–18]

2.5 | Redox Potentials

Cyclic voltammetry experiments were carried out to measure the redox potentials (E_{ox} and E_{red}) of KCs using tetrabutylammonium hexafluorophosphate (0.1 M) as the supporting electrolyte in acetonitrile (potential vs. saturated calomel electrode). The free energy change (ΔG_{et}) for an electron transfer reaction was calculated according to Equation (1),[19] where E_{ox}, E_{red}, and E^* stand for the oxidation potential of the electron donor, the reduction potential of the electron acceptor, and the excited-state energy (E_{S1} or E_{T1}). C is the coulombic term for the initially formed ion pair (usually neglected in polar solvents).

$$\Delta G_{et} = E_{ox} - E_{red} - E^* + C. \quad (1)$$

2.6 | ESR Spin-Trapping Experiments

The electron spin resonance spin-trapping (ESR-ST) experiments were carried out using an X-band spectrometer (Magnettech MS400). *Tert*-butylbenzene was selected as a solvent. LED@405 nm was used as irradiation source for the generation of radicals at room temperature under N_2; these latter were trapped by phenyl-*N*-*tert*-butylnitrone (PBN) according to a procedure described elsewhere in detail.[17,18] The ESR spectra simulations were carried out with the PEST WINSIM program.

2.7 | UV–Visible Absorption and Photolysis Experiments

JASCO V730 UV–visible spectrometer was used to study the absorbance properties of the different compounds investigated in this research as well as the steady-state photolysis experiments.

2.8 | Fluorescence Experiments

A JASCO FP-6200 spectrofluorimeter was used to study the fluorescence properties of the compounds as well as their fluorescence quenching data.

2.9 | Computational Procedure

The frontier orbitals (highest occupied molecular orbital [HOMO] and lowest unoccupied molecular orbital

[LUMO]) were calculated at Density Functional Theory (DFT) level (UB3LYP/6-31G*). The UV–vis spectra were calculated at DFT level. The triplet state energy was evaluated after full geometry optimization of S_0 and T_1. The computational procedure was reported by us in Reference [20].

2.10 | 3D Printing Experiments Using Laser Diode

For 3D printing experiments, a laser diode @405 nm (spot size of 50 μm) was used as irradiation source. The photosensitive resins (various thickness) were polymerized under air and the generated 3D patterns were characterized by numerical optical microscopy (DSX-HRSU from OLYMPUS Corporation) as presented by us in References [21, 22].

2.11 | Near-UV Conveyor

The Dymax near-UV conveyor was used to cure composites. The glass fibers were impregnated with the organic resin (50/50 w/w%) and then irradiated. The near-UV conveyor is equipped with a 120 mm wide Teflon-coated belt and a LED @395 nm (4 W cm^{-2}). The distance between the LED and the belt can be adjusted (fixed at 15 mm); the belt speed was 2 m min^{-1}.

3 | RESULTS AND DISCUSSION

3.1 | Synthesis of the Coumarins and KCs Compounds

Coumarin **Coum-A1** was synthetized according to reported procedure[23] (see Supporting Information for procedure details) by condensation of 4-diethylaminosalicylaldehyde with 2-(4-nitrophenyl)acetonitrile catalyzed by piperidine, followed by hydrolysis in acidic medium (see Scheme 2).

Suzuki-Miyaura coupling reaction is a valuable process for the preparation of 3-aryl-coumarin scaffold.[24] Appling this methodology **Coum-B1** was synthetized starting from 3-bromo-7-diethylamino coumarin and 4-(dimethylamino)benzeneboronic acid, both easily prepared from commercially available materials (Scheme 3) (see Supporting Information for procedure details).

The KC is easily synthetized by the Knoevenagel condensation of salicylaldehyde derivatives with β-ketoesters catalyzed by piperidine (Scheme 4).[2] The reaction could be conducted in ethanol at reflux temperature (for **KC-C**

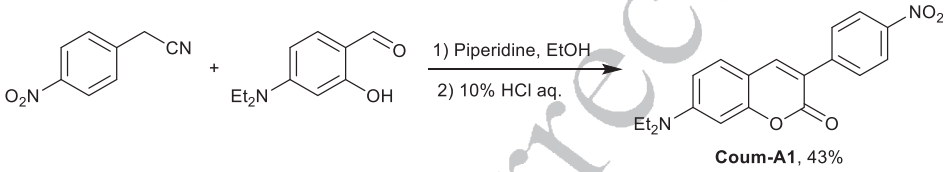

SCHEME 2 Synthetic procedure for the investigated compounds (**Coum-A1**)

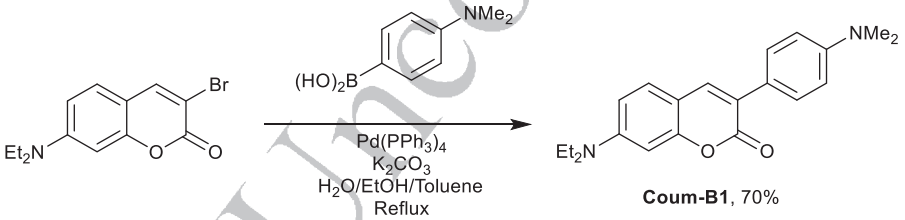

SCHEME 3 Synthetic procedure for the investigated compounds (**Coum-B1**)

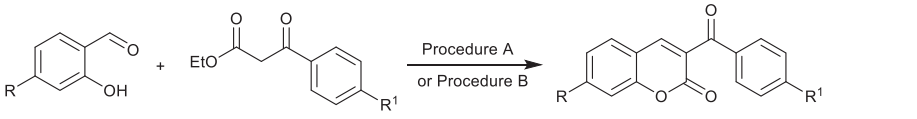

Procedure A: piperidine (cat.), EtOH, reflux
Procedure B: piperidine (cat.), neat, r.t.

KC-C, R = $N(Et)_2$, R^1 = H; 43% (procedure A)
KC-D, R = $N(Et)_2$, R^1 = F; 48% (procedure A)
KC-E, R = OMe, R^1 = H; 65% (procedure B)
KC-F, R = $N(Et)_2$, R^1 = OMe; 69% (procedure B)
KC-G, R = H, R^1 = OMe; 47% (procedure B)
KC-H, R = H, R^1 = $N(Me)_2$; 76% (procedure B)

SCHEME 4 Synthetic procedure for the investigated compounds (**KC-C, KC-D, KC-E, KC-F, KC-G,** and **KC-H**)

and **KC-D**) or in solvent-less conditions at room temperature (for **KC-E**, **KC-F**, **KC-G**, **KC-H**) provides a "green" alternative to coumarin synthesis (see Supporting Information for procedure details).

3.2 | Light Absorption Properties of the Investigated Compounds

As expected, high molar extinction coefficients characterized the different KCs in the near UV and the visible range, for example, $\varepsilon_{(KC\text{-}C)}$ = 39,060 M^{-1} cm^{-1} at λ_{max} = 422 nm, $\varepsilon_{(KC\text{-}F)}$ = 35,440 M^{-1} cm^{-1} at λ_{max} = 416 nm (Table 1 and Figure 2). It is well obvious that the absorptions of the KC derivatives are extremely high in the 270–560 spectral range providing a great overlap with the emission spectra of the near UV or visible light sources (e.g., LED@375 or 405 nm).

TABLE 1 Parameters characterizing the light absorption properties of coumarins and KCs: maximum absorption wavelengths λ_{max}, extinction coefficients at λ_{max}, and extinction coefficients at the emission wavelength of the LED@405 nm

PI	λ_{max} (nm)	ε_{max} (M^{-1} cm^{-1})	$\varepsilon_{@405nm}$ (M^{-1} cm^{-1})
Coum-A1	432	29,770	**21,600**
Coum-B1	407	23,250	**23,200**
KC-C	422	39,060	**31,730**
KC-D	423	31,380	**24,810**
KC-E	343	17,590	**260**
KC-F	416	35,440	**32,420**
KC-G	294	18,740	**160**
KC-H	349	22,370	**3,260**

Abbreviations: KC, keto-coumarin; LED, light-emitting diode.

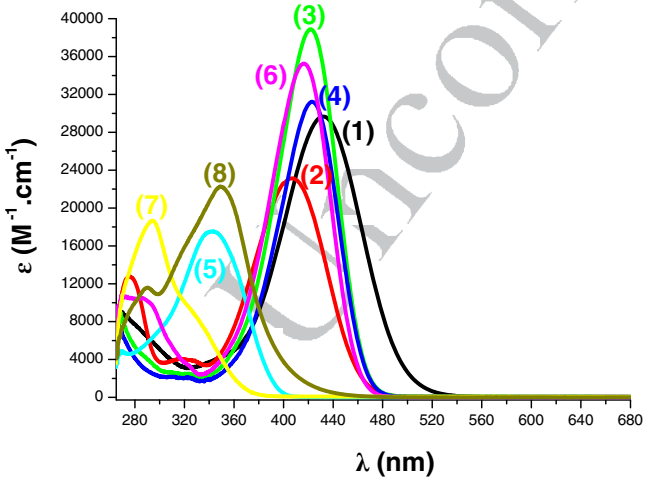

FIGURE 2 Absorption spectra of the investigated compounds in acetonitrile: (1) **Coum-A1**; (2) **Coum-B1**; (3) **KC-C**; (4) **KC-D**; (5) **KC-E**; (6) **KC-F**; (7) **KC-G**; and (8) **KC-H** [Color figure can be viewed at wileyonlinelibrary.com]

The optimized geometries as well as the frontier orbitals (i.e., HOMO and LUMO) for the different KCs are depicted in Figure 3. It is well obvious that both the HOMOs and LUMOs are delocalized on the π system leading to a $\pi \rightarrow \pi^*$ lowest energy transition. A partial charge transfer transition character can also be observed for some derivatives (e.g., **KC-H**, **KC-D**) with HOMO and LUMO localized on different part of the molecule.

3.3 | CP of Epoxides

The CP of epoxides was investigated first in the presence of the new synthesized KC derivatives. In order to use safe and cheap source of irradiation, the LED @405 nm was chosen as visible light irradiation for this study. Interestingly, good polymerization efficiencies for the CP of epoxides were observed when using two-component PISs based on the different KC/Iod couples (0.2%/1% w/w), for example, FC = 45% for **KC-C** (Figure 4a, curve 1 and Table 2). A new peak appears at ~1,080 cm^{-1} in the FTIR spectra in the course of the polymerization ascribed to the formation of the polyether network (see Figure 4b). In the same conditions, using Iod or KC alone does not lead to any polymerization clearly showing that the presence of KC is required for an efficient process. Therefore, a favorable photo-oxidation process can take place in the presence of these compounds when combined with an Iod salt as the additive (see the chemical mechanisms in Section 3.7).

When taking into account the photopolymerization results of KCs, the light absorption properties of these compounds appear to be a very important parameter corresponding to a key factor of their efficiency, that is, the polymerization rates upon irradiation @405 nm follow the order: **KC-C** > **KC-F** > **KC-D** > **KC-H** > **KC-E** >> **KC-G** which is in line with their respective absorption properties ($\varepsilon_{@405\ nm}$; Table 1). Therefore, a better light absorption is useful to convert light more efficiently to initiating species. A difference of reactivity between the different generated radical cations ($KC^{\bullet+}$) must also be taken into account to explain the better initiating ability of such compounds (see the chemical mechanisms below). A third parameter that may be responsible for the different initiation efficiency is the formation of Brønsted acid as initiating species.[9]

Color online, B&W in print

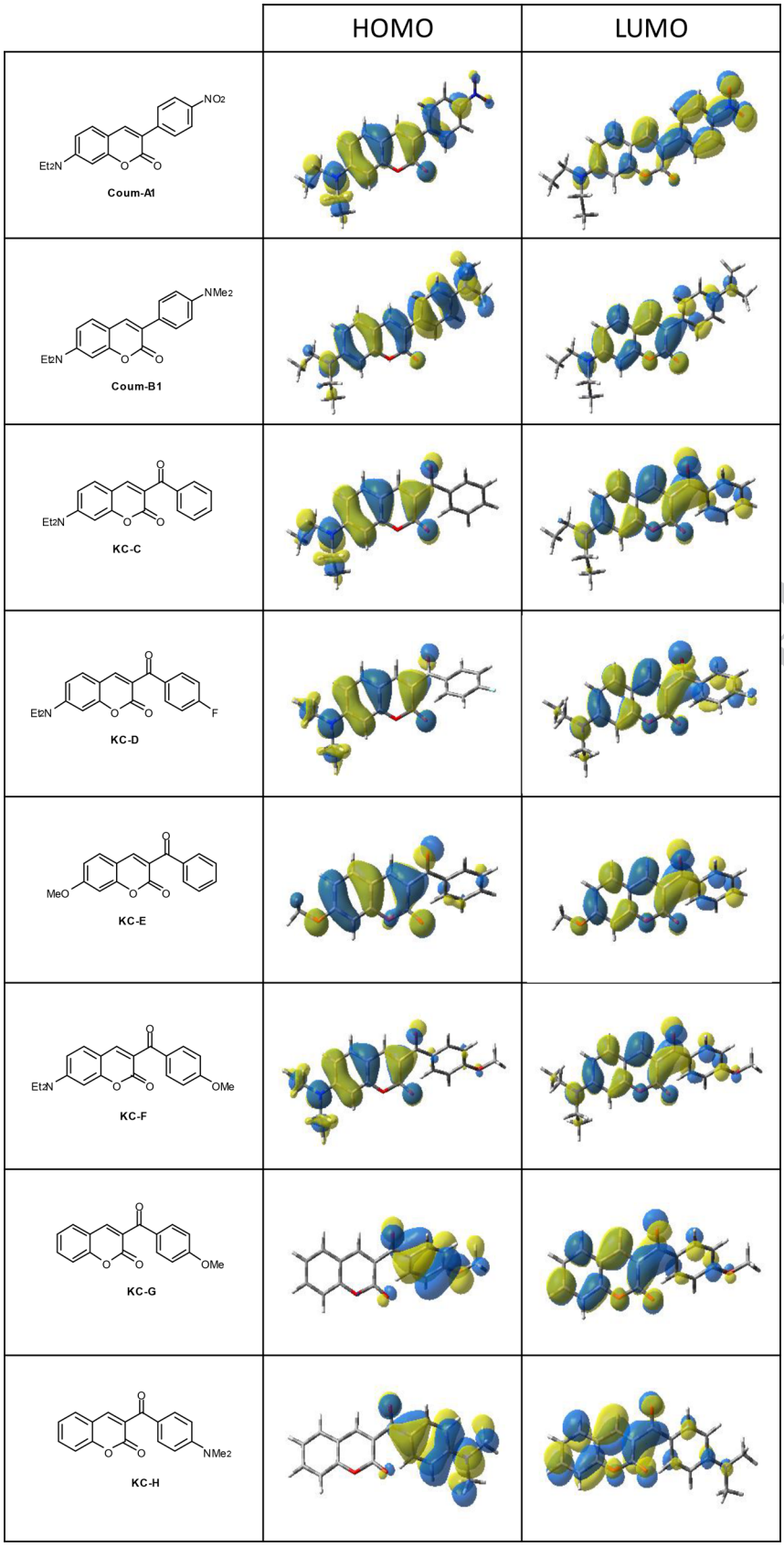

FIGURE 3 Contour plots of highest occupied molecular orbitals and lowest unoccupied molecular orbitals for coumarins and keto-coumarin compounds; structures optimized at the B3LYP/6-31G* level of theory [Color figure can be viewed at wileyonlinelibrary.com]

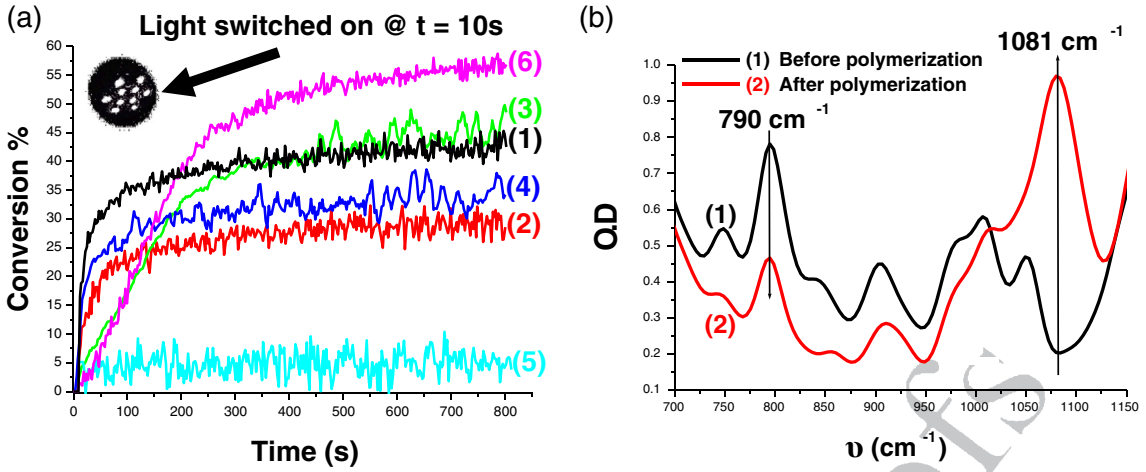

Color online; B&W in print

FIGURE 4 (a) Polymerization profiles (epoxy function conversion vs. irradiation time) of 25 μm thin epoxide films under air upon exposure to the LED@405 nm in the presence of the two-component photoinitiating systems based on keto-coumarin (KC) compounds: (1) **KC-C**/Iod (0.2%/1% w/w); (2) **KC-D**/Iod (0.2%/1% w/w); (3) **KC-E**/Iod (0.2%/1% w/w); (4) **KC-F**/Iod (0.2%/1% w/w); (5) **KC-G**/Iod (0.2%/1% w/w); and (6) **KC-H**/Iod (0.2%/1% w/w). The irradiation starts for $t = 10$s. (b) IR spectra recorded before and after polymerization of epoxide film using **KC-C**/Iod (0.2%/1% w/w) upon irradiation with the LED@405 nm [Color figure can be viewed at wileyonlinelibrary.com]

TABLE 2 Final reactive epoxy FC for EPOX using different two-component PISs after 800 s of irradiation with the LED @405 nm

KC/Iod (0.2%/1% w/w) (thickness = 25 μm) under air					
KC-C/Iod (%)	**KC-D/Iod (%)**	**KC-E/Iod (%)**	**KC-F/Iod (%)**	**KC-G/Iod**	**KC-H/Iod (%)**
45	31	50	38	n.p.	59

Abbreviations: Iod, iodonium; FC, function conversion; KC, keto-coumarin; LED, light-emitting diode; n.p.: no polymerization; PIS, photoinitiating system.

3.4 | Free-radical photopolymerization of Acrylates (TMPTA)

The free-radical polymerization (FRP) of TMPTA films, in the presence of the different two or three-component PISs (KC/Iod, KC/NPG, KC/EDB, or KC/Iod/NPG) based on KC derivatives, was carried in laminate and upon irradiation with the LED @405 (Figure 5 and Table 3). The photopolymerization process was very efficient in terms of both final acrylate function conversion (FC) but also rate of polymerization (R_p). When testing Iod, NPG, or EDB alone under the same irradiation conditions, no polymerization took place clearly highlighting the huge role of KCs for the global performance of the system.

First starting with the photo-oxidation process, the KC/Iod couples efficiently initiate the FRP of acrylates as shown in Figure 5a. According to the experimental results, it is quite obvious that **KC-C** and **KC-F** are the most effective PIs when combined with the Iod salt (Figure 5a, curves 2 and 5). This behavior can be related to their highest extinction coefficients @405 nm ($\varepsilon_{(@405\ nm)}$ = 31,730 M^{-1} cm^{-1} for **KC-C** and 32,420 M^{-1} cm^{-1} for **KC-F**; Table 1).

In the same context, good polymerization profiles for the FRP of thick samples (1.4 mm) can also be obtained with the LED @405 nm under air (Figure 6a; see also the FCs in Table 3). The efficiency trend for thick samples follows the trend obtained above for thin films (i.e., **KC-C > KC-F > KC-D > KC-E > > KC-G, KC-H)**. This trend obeys to the respective light absorption properties of these derivatives.

On the other hand, when replacing the Iod salt by NPG, KC derivatives are able to efficiently initiate the FRP of thin and thick TMPTA samples (Figures 5b and 6b) showing that these compounds are also excellent type II PIs for a photo-reduction process using NPG as a co-initiator. Both high final acrylate FC and also R_p were achieved with such compounds (Figures 5b and 6b and Table 3). For thin films, the efficiency trend follows the order: **KC-C > KC-F > KC-D > KC-E > KC-G > KC-H** which is directly connected to their absorption properties. Whereas for thick TMPTA samples, the observed trend (**KC-E > KC-F > KC-C > KC-D > KC-G > > KC-H)** does not follow their light absorption and can be related to inner filter effect which takes place during the photopolymerization process. This latter phenomenon was

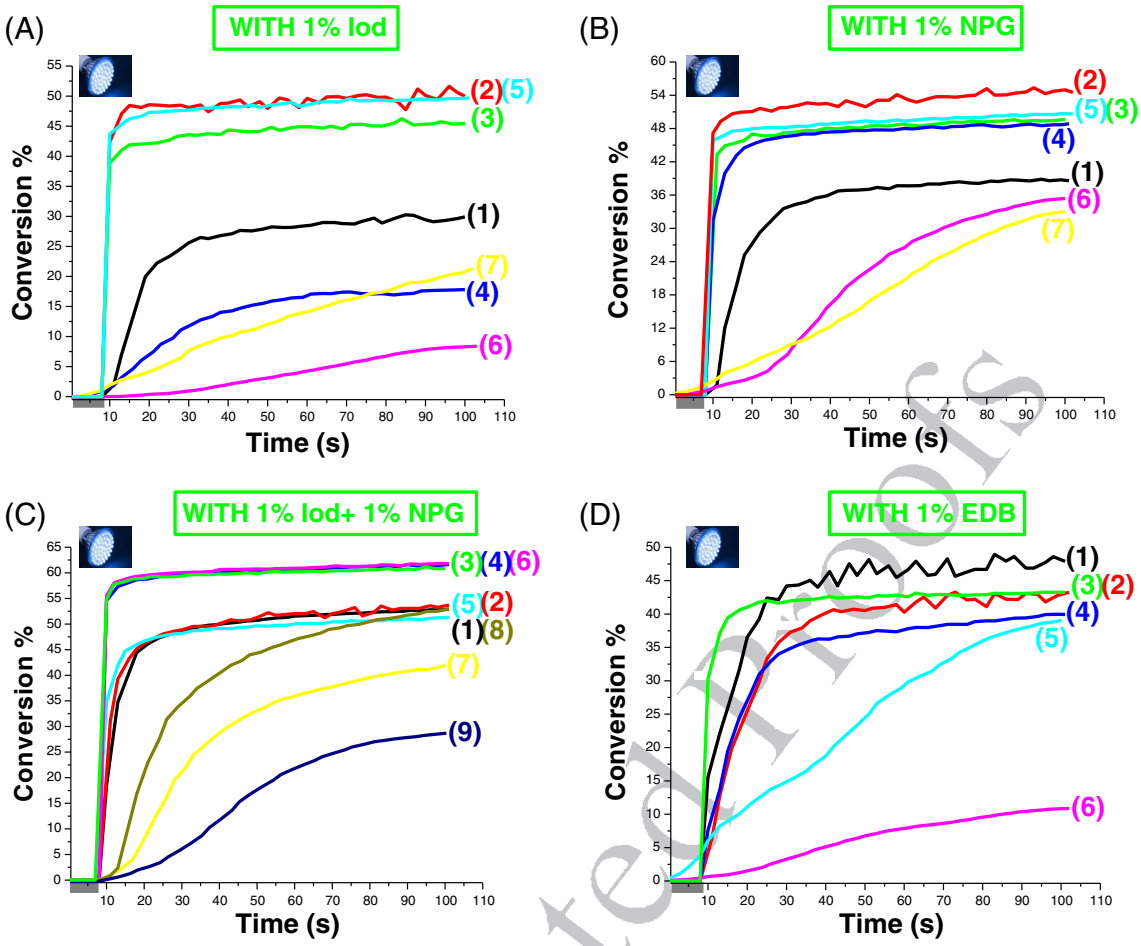

Color online, B&W in print

FIGURE 5 Polymerization profiles (acrylate function conversion vs. irradiation time) of 25 μm thin trimethylolpropane triacrylate films, in laminate upon irradiation with the LED@405 nm in the presence of different two and three-component photoinitiating systems: (a) **PI/Iod (0.2%/1% w/w):** (1) Coum-A1/Iod; (2) KC-C/Iod; (3) KC-D/Iod; (4) KC-E/Iod; (5) KC-F/Iod; (6) KC-G/Iod; and (7) KC-H/Iod. (b): **PI/NPG (0.2%/1% w/w):** (1) Coum-A1/NPG; (2) KC-C/NPG; (3) KC-D/NPG; (4) KC-E/NPG; (5) KC-F/NPG; (6) KC-G/NPG; and (7) KC-H/NPG. (c) **PI/Iod/NPG (0.2%/1%/1% w/w):** (1) Coum-A1/Iod/NPG; (2) Coum-B1/Iod/NPG; (3) KC-C/Iod/NPG; (4) KC-D/Iod/NPG; (5) KC-E/Iod/NPG; (6) KC-F/Iod/NPG; (7) KC-G/Iod/NPG; (8) KC-H/Iod/NPG.; and (9) Iod/NPG (1%/1% w/w). (d) **PI/EDB (0.2%/1% w/w):** (1) KC-C/EDB; (2) KC-D/EDB; (3) KC-E/EDB; (4) KC-F/EDB; (5) KC-G/EDB; and (6) KC-H/EDB [Color figure can be viewed at wileyonlinelibrary.com]

fully confirmed by the calculations of the KC absorbances (@405 nm) according to Beer–Lambert law (A (@405 nm) = ε(@405 nm).l.C) (Table 4). From these data, it is obvious that **KC-E** which presents the lowest absorbance among its series allows more penetration of light compared to the other derivatives making it at the top of the list in the efficiency trend ($A_{(\mathbf{KC\text{-}E})}$ = 0.3 vs. 26.7! for **KC-C**; Table 4). Consequently, important inner filter effect is expected for **KC-C** for thick samples for the investigated concentration.

Otherwise, when comparing KC/NPG versus KC/EDB couples, we notice a difference of order in the trend of efficiency. This will be explained below by less favorable electron transfer with EDB compared to NPG, that is, the electron transfer quantum yields (ϕ_{et}) obtained with EDB are lower than for NPG ($\phi_{et(EDB)}$ = 0.16 for **KC-C** vs. 0.97 with NPG; $\phi_{et(EDB)}$ = 0.18 vs. $\phi_{et(NPG)}$ = 0.96 for **KC-F**; Table 5).

Moreover, excellent polymerization profiles were observed for the three-component (KC/Iod/NPG) PISs. The addition of the amine (NPG) as a hydrogen donor leads to an increase of the system performance in terms of both FC and R_p compared to the KC/Iod systems (e.g., FC increases up to reach 62% for **KC-D**/Iod/NPG [0.2%/1%/1% w/w] compared to 46% for **KC-D**/Iod [0.2%/1% w/w]; Figure 5a,c and Table 3). For comparison purposes, the two-component system Iod/NPG (1%/1% w/w) was tested and it shows very low polymerization ability (Figure 5c, curve 9), highlighting the tremendous role of the KC derivatives for the overall performance of

TABLE 3 Final reactive acrylate FC for TMPTA using different two (0.2%/1% w/w) and three-component PISs (0.2%/1%/1% w/w) after 100 s of irradiation with the LED @405 nm

	Thin sample (25 μm) in laminate				Thick sample (1.4 mm) under air			
	Two-component PIS			Three-component PIS	Two-component PIS			Three-component PIS
	+Iod (%)	+NPG (%)	+EDB (%)	+Iod/NPG (%)	+Iod (%)	+NPG (%)	+EDB (%)	+Iod/NPG (%)
Coum-A1	30	39		53	n.p.	n.p.		n.p.
Coum-B1				54				79
KC-C	52	55	49	61	67	77	n.p.	83
KC-D	46	50	44	62	62	71	n.p.	82
KC-E	18	49	44	52	37	86	83	86
KC-F	50	51	40	62	69	82	n.p.	86
KC-G	n.p.	36	39	42	n.p.	78	54	83
KC-H	n.p.	33	n.p.	53	n.p.	n.p.	n.p.	n.p.

Abbreviations: EDB, ethyl 4-(dimethylamino)benzoate; FC, function conversion; Iod, iodonium; KC, keto-coumarin; LED, light-emitting diode; n.p. no polymerization; NPG, *N*-phenylglycine; PIS, photoinitiating system; TMPTA, trimethylolpropane triacrylate.

the system. The same behavior was also observed in the presence of the others KCs for the three-component (KC/Iod/NPG) PISs compared to the two component PISs (Figure 5c vs. Figure 5a, respectively; Table 3).

For thick samples, the three-component (KC/Iod/NPG) PISs are also characterized by better performance than the two-component ones (e.g., the efficiency rises up to attain 86% for **KC-F**/Iod/NPG [0.2%/1%/1% w/w] vs. 69% for **KC-F**/Iod [0.2%/1% w/w]; Figure 6a,c and Table 3).

For the comparison between KC and coumarin derivatives, KCs show better performance than the coumarin derivatives. As evidenced in Figure 5a,b, respectively, **Coum-A1**/Iod or NPG show lower efficiencies compared to that obtained with the KC derivatives. For the three-component PISs, **Coum-A1** (or **Coum-B1)**/Iod/NPG exhibits rather similar performance than **KC-E** but lower performance than those derived from **KC-C**, **KC-D**, and **KC-F** (Figure 5c). Furthermore, **Coum-A1**/Iod or **Coum-A1**/NPG (0.2%/1% w/w) couples and **Coum-A1**/Iod/NPG (0.2%/1%/1% w/w) combination were tested for the FRP of TMPTA in thick films using LED@405 nm and almost no polymerization occurs (Figure 6a–c). A similar behavior was obtained for **Coum-B1**/Iod/NPG (0.2%/1%/1% w/w) and Iod/NPG (0.2%/1% w/w) as shown in Figure 6c (curve 2 and curve 9, respectively). These behaviors suggested that investigated KCs are better than coumarins.

Compared to well-established structures (e.g., phosphine-oxide Type I PI like Irgacure 819), the new proposed systems are quite efficient (maximum conversion reached in less than 10s as for this reference PI).

3.5 | Laser Write Experiments for the Access to 3D Generated Patterns Using KC/NPG, KC/EDB, or KC/Iod/NPG Combinations

Laser write experiments were successfully carried out under air upon laser diode irradiation (@405 nm) for different two (KC/NPG or EDB) or three-component (KC/Iod/NPG) PISs for acrylates (TMPTA). Using this technique, we were able to prepare thick polymer samples in a very short time scale (<1 min) and with a very high spatial resolution (only limited by the size of the laser diode beam: spot of 50 μm). Numerical optical microscopy experiments were used to characterize the 3D-generated patterns and the results are illustrated in Figures 7 and S1.

3.6 | LED Conveyor Experiments for the Photocomposites Synthesis

The very good efficiency of KCs to initiate the polymerization of acrylates prompts us to use them for the preparation of photocomposites which are well known for their improved mechanical properties. Recently, composites have become dominant emerging materials owing to the fact that they are characterized by several interesting properties which are strongly required for industrial applications. Among these properties: lightweight, high strength, corrosion, and chemical resistance.

In this work, the preparation of photocomposites requires the impregnation of the glass fibers by an organic

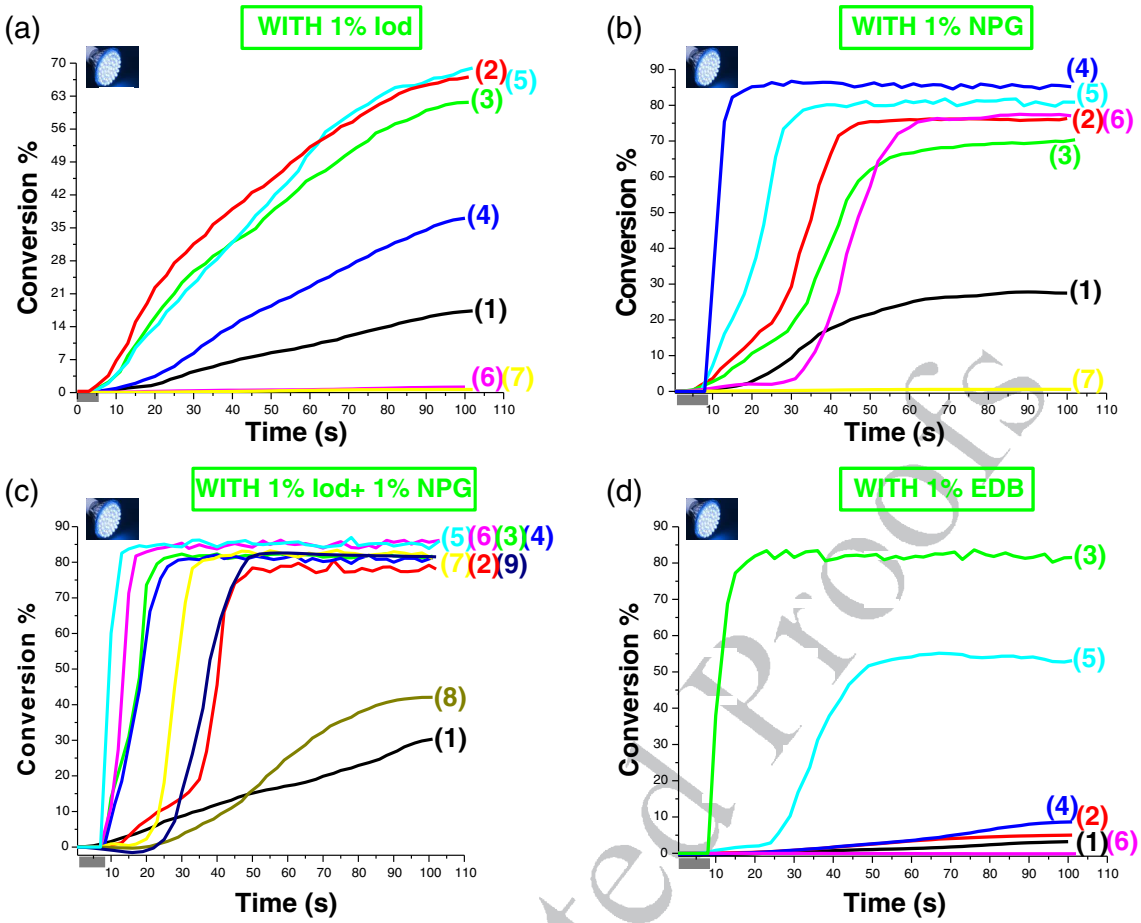

Color online, B&W in print

FIGURE 6 Polymerization profiles (acrylate function conversion vs. irradiation time) for 1.4 mm thick samples of trimethylolpropane triacrylate (under air, using LED@405 nm) in the presence of different two and three-component photoinitiating systems: (a) **PI/Iod (0.2%/1% w/w):** (1) Coum-A1/Iod; (2) KC-C/Iod; (3) KC-D/Iod; (4) KC-E/Iod; (5) KC-F/Iod; (6) KC-G/Iod; and (7) KC-H/Iod. (b): **PI/NPG (0.2%/1% w/w):** (1) Coum-A1/NPG; (2) KC-C/NPG; (3) KC-D/NPG; (4) KC-E/NPG; (5) KC-F/NPG; (6) KC-G/NPG; and (7) KC-H/NPG. (c) **PI/Iod/NPG (0.2%/1%/1% w/w):** (1) Coum-A1/Iod/NPG; (2) Coum-B1/Iod/NPG; (3) KC-C/Iod/NPG; (4) KC-D/Iod/NPG; (5) KC-E/Iod/NPG; (6) KC-F/Iod/NPG; (7) KC-G/Iod/NPG; (8) KC-H/Iod/NPG.; and (9) Iod/NPG (1%/1% w/w). (d) **PI/EDB (0.2%/1% w/w):** (1) KC-C/EDB; (2) KC-D/EDB; (3) KC-E/EDB; (4) KC-F/EDB; (5) KC-G/EDB; and (6) KC-H/EDB [Color figure can be viewed at wileyonlinelibrary.com]

TABLE 4 Extinction coefficients and absorbances at the emission wavelength of the LED@405 nm for a thick sample

PI	$\varepsilon_{@405nm}$ (M^{-1} cm^{-1})	$A_{@405nm}$
KC-C	31,730	**26.7**
KC-D	24,810	**20.5**
KC-E	260	**0.3**
KC-F	32,420	**27.2**

Abbreviations: KC, keto-coumarin; LED, light-emitting diode; PI, photoinitiator.

resin (50% glass fibers/50% resin w/w) and then by irradiating the sample with the LED@395 nm; TMPTA-based organic resin has been used for this study. The photos before and after irradiation are depicted in Figures 8 and S2. The experimental results show that the KCs were able to completely cure composites where only one pass of irradiation at the surface is required to be tack-free (for 2 m min^{-1} belt speed) and within one or few passes for the bottom of the sample (one layer of glass fibers; thickness = 2 mm). The results obtained are gathered in Table S1. Otherwise, we noted that in most of the time the color of the initial composition remains light colored, but sometimes a light brown color appeared after irradiation.

3.7 | Chemical Mechanisms

3.7.1 | Steady-State Photolysis

The study of the steady-state photolysis experiments for the different KC-based systems has been carried out

TABLE 5 Parameters characterizing the photochemical mechanisms associated with ^{1,3}Coumarin or ^{1,3}KC/Iod, ^{1,3}Coumarin or ^{1,3}KC/NPG, and ^{1,3}Coumarin or ^{1,3}KC/EDB in acetonitrile

PI	E_{S1} (eV)	E_{T1} (eV)[a]	E_{ox} (eV)	$\Delta G_{et(S1)}$ [b 1] (PI/Iod) (eV)	$\Delta G_{et(T1)}$ [b 3] (PI/Iod) (eV)	K_{SV} (PI/Iod) (M^{-1})	$\phi_{et(S1)}$ [c] (PI/Iod)	K_{SV} (PI/NPG) (M^{-1})	$\phi_{et(S1)}$ [c] (PI/NPG)	K_{SV} (PI/EDB) (M^{-1})	$\phi_{et(S1)}$ [c] (PI/EDB)
Coum-A1	2.68	1.97	1.19	−1.29	−0.58	—	—	<0	—	<0	—
Coum-B1	2.67	1.96	0.71	−1.76	−1.05	87.81	0.62	43.84	0.74	—	—
KC-C	2.7	2.17	1.28	−1.22	−0.69	9.68	0.15	432.68	0.97	3.69	0.16
KC-D	2.7	2.26	0.36	−2.14	−1.7	—	—	49.77	0.77	—	—
KC-E	3.02	2.37	0.46	−2.36	−1.71	157.44	0.75	11.35	0.43	—	—
KC-F	2.73	2.27	1.38	−1.15	−0.69	13.34	0.2	353.23	0.96	4.29	0.18
KC-G	3.67	2.41	0.46	−3.01	−1.75	13.43	0.2	1064.53	0.99	—	—
KC-H	3.74	2.29	1.38	−2.16	−0.71	—	—	<0	—	—	—

Abbreviations: EDB, ethyl 4-(dimethylamino)benzoate; Iod, iodonium; KC, keto-coumarin; NPG, *N*-phenylglycine; PI, photoinitiator.

[a]Calculated triplet state energy level at DFT level.

[b]For Iod, a reduction potential of −0.2 eV was used for the ΔG_{et} calculations.[9]

[c]From eq. 2 presented in Reference [9].

using UV–visible spectroscopy. As shown in Figure 9, a very fast photolysis was observed for **KC-F** in the presence of Iod salt upon irradiation with the LED@375 nm compared to the very high photostability of **KC-F** alone for which no photolysis occurs (**KC-F**/Iod in Figure 9b vs. **KC-F** alone in Figure 9a). This photolysis clearly suggests a strong **KC-F**/Iod interaction. Furthermore, an isobestic point at about 353 nm is found in the **KC-F**/Iod photolysis indicating that no other secondary reaction occurs. The interaction that takes place between **KC-F** and Iod salt leads to a clear consumption of **KC-F** which is shown in Figure 9c, where the optical density of the solution is measured in the presence of Iod (curve 2 in Figure 9c) or without Iod (curve 1 in Figure 9c) at different time of irradiation. A similar behavior is observed for **KC-C** and **KC-D** in the presence of Iod, that is, very high photolysis are noticed with Iod versus high photostability of the compound alone. Otherwise, for **KC-E**, **KC-G** or **KC-H**, no or very low photolysis in the presence of Iod was observed.

3.7.2 | Excited-State Reactivity

Fluorescence and fluorescence quenching experiments for the different KCs involved in this work have been carried out in acetonitrile using fluorescence spectroscopy. The obtained results are illustrated in Figure 10. In fact, the crossing point between the absorption and the fluorescence spectra allows the determination of the singlet excited-state energy for the different compounds studied, for example, $E_{S1} = 2.73$ eV for **KC-F** (Table 5).

The free energy changes (ΔG_{et}) for the electron transfer reaction which occurs between KCs as electron donors and Iod as electron acceptor were calculated according to Equation (1) using the oxidation potentials E_{ox} and the excited-state energies (E_{S1} or E_{T1}) of KCs (Table 5). Favorable fluorescence quenching processes of ^{1}**KC-F** (and generally ^{1}KC) by Iod salt are shown in full agreement with the favorable calculated values of the free energy change ($\Delta G_{et(KC/Iod)}$) (r1 and r2 in Scheme 5; e.g., for ^{1}**KC-F**/Iod, $\Delta G_{et(S1)} = -1.15$ eV; Table 5); the potential of the first oxidation peak of Coumarins and KCs is determined by cyclic voltammetry (for KC-F; E_{ox} ~1,38 V, see Table 5, see also Figure S3 in SI for the other KCs).

$$\phi_{et} = K_{sv}[Iod]/(1 + K_{sv}[Iod]). \quad (2)$$

The interaction between KCs and Iod salt can also occur via triplet excited states, that is, this is confirmed by the favorable values of the free energy change ($\Delta G_{et(T1)}$) for the electron transfer reaction ^{3}KC/Iod, for

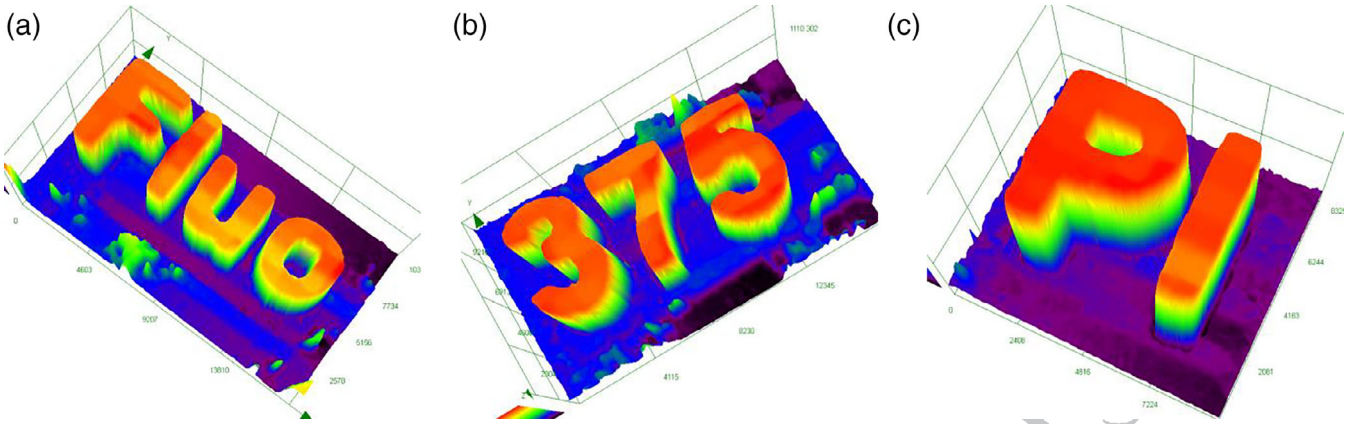

Color online, B&W in print

FIGURE 7 Free-radical photopolymerization experiments for laser write upon laser diode irradiation: characterization of the 3D written patterns by numerical optical microscopy; (a) **KC-D**/Iod/NPG (0.02%/0.1%/0.1% w/w) in trimethylolpropane triacrylate (TMPTA) (thickness = 2,220 μm); (b) **KC-C**/Iod/NPG (0.016%/0.083%/0.083% w/w) in TMPTA (thickness = 2,220 μm); and (c) **KC-C**/NPG (0.025%/0.125% w/w) in TMPTA (thickness = 1,590 μm for (a)); respectively [Color figure can be viewed at wileyonlinelibrary.com]

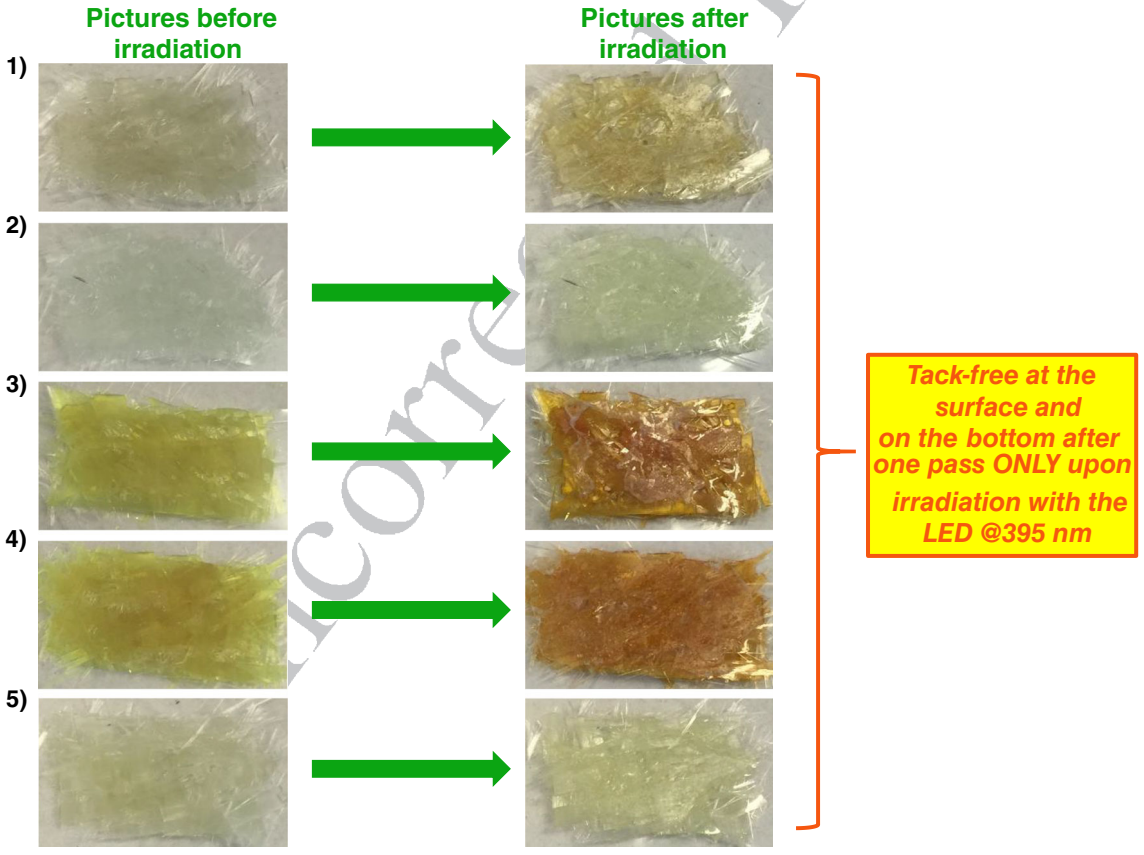

Color online, B&W in print

FIGURE 8 Photocomposites produced upon Near-UV light (LED@395 nm), Belt Speed = 2 m/min, using the free-radical polymerization in the presence of 50% glass fibers/50% acrylate resin (thickness = 2 mm for one layer of glass fibers) for different systems: (1) 0.2% **KC-E** + 1% Iod + 1% NPG in trimethylolpropane triacrylate (TMPTA); (2) 0.2% **KC-E** + 1% EDB in TMPTA; (3) 0.2% **KC-F** + 1% Iod + 1% NPG in TMPTA; (4) 0.2% **KC-C** + 1% Iod + 1% NPG in TMPTA; and (5) 0.2% **KC-E** + 1% NPG in TMPTA [Color figure can be viewed at wileyonlinelibrary.com]

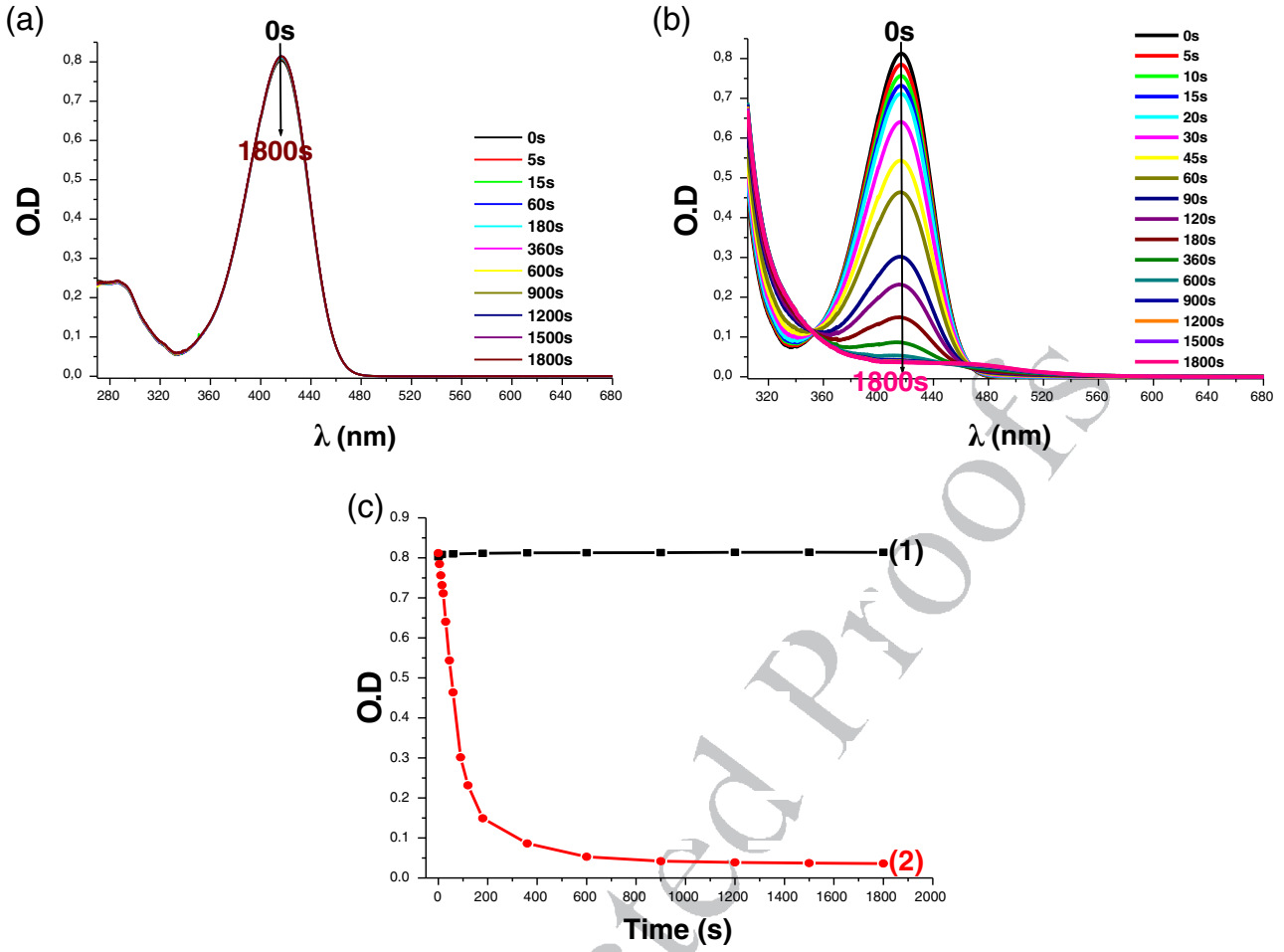

Color online, B&W in print

FIGURE 9 (a) Photolysis of **KC-F** alone; (b) **KC-F**/Iod photolysis; and (c) photodegradation of **KC-F** without (1) and with (2) iodonium salt versus irradiation time, upon exposure to the LED @375 nm in acetonitrile [Color figure can be viewed at wileyonlinelibrary.com]

example, for **KC-D**: $\Delta G_{et(T1)} = -1.7$ eV versus $\Delta G_{et(S1)} = -2.14$ eV (Table 5).

To better understand the interactions that take place, a global proposed mechanism is provided and presented in Scheme 5 (r1–r8) according to References [25, 26]. ESR results confirm completely these proposed chemical mechanisms by establishing the detection of aryl radicals.[9] Indeed, the aryl radicals ($Ar^{\bullet}$) can be easily detected as radical adducts PBN/$Ar^{\bullet}$ in the irradiated solution of KC/Iod in ESR-ST experiments. In fact, these radical adducts (PBN/$Ar^{\bullet}$) are characterized by typical hyperfine coupling constants (hfcs): $a_N = 14.1$ G and $a_H = 2.1$ G in full agreement with reported data.[27] Remarkably, for addition onto methyl acrylate double bond, the aryl radicals are considered among the most efficient initiating species ($k_{add} \sim 10^8$ M^{-1} s^{-1})[9] suitable with the good efficiency of the KCs/Iod couples to act as radical PIs.

On the other hand, it is proposed that a charge transfer complex (CTC) can be formed between NPG which is an *N*-aromatic electron donor and Iod salt which is an electron poor (r3) as what was very recently published.[28] This $[NPG\text{-}Iod]_{CTC}$ structure is quite convenient as it provides an enhanced visible light absorption to the PIS. In addition, the photolysis of this latter structure at 405 nm leads to an efficient release of aryl radicals $Ar^{\bullet}$ (r4) as confirmed by the photopolymerization study (curve 9 in Figures 5c and 6c).

Moreover, for the interaction that took place between KCs and NPG, an electron/proton transfer reaction can be proposed (r1 and r5). A decarboxylation reaction (r6) which leads to the formation of $NPG_{(-H;-CO2)}^{\bullet}$ is suggested to avoid any back of electron transfer reaction.[9] Therefore, ($NPG_{(-H;-CO2)}^{\bullet}$) can be considered as the initiating species for the FRP in the presence of KC/NPG systems.

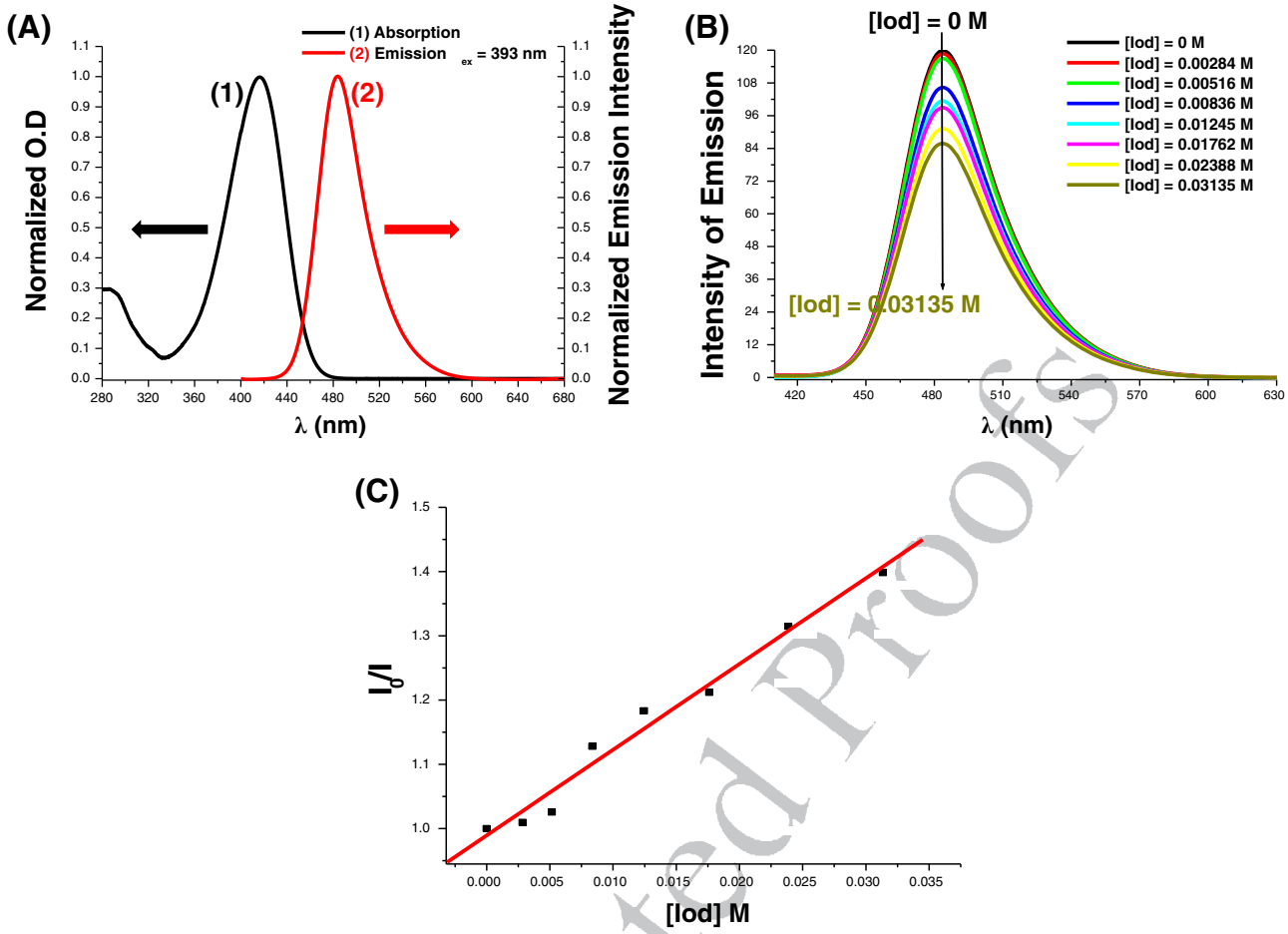

Color online, B&W in print

FIGURE 10 (a) Singlet state energy determination in acetonitrile for **KC-F**; (b) fluorescence quenching of **KC-F** by Iod; and (c) Stern–Volmer treatment for the **KC-F**/Iod fluorescence quenching [Color figure can be viewed at wileyonlinelibrary.com]

$$KC \rightarrow {}^{*}KC\ (h\nu) \quad (r1)$$

$${}^{*}KC + Ar_2I^{+} \rightarrow KC^{\bullet+} + Ar_2I^{\bullet} \quad (r2A)$$

$$KC^{\bullet+} + Ar_2I^{\bullet} \rightarrow KC^{\bullet+} + Ar^{\bullet} + ArI \quad (r2B)$$

$$NPG + Iod \rightarrow [NPG\text{-}Iod]_{CTC} \quad (r3)$$

$$[NPG\text{-}Iod]_{CTC} \rightarrow\rightarrow\rightarrow Ar^{\bullet} \quad (h\nu) \quad (r4)$$

$${}^{*}Keto\text{-}coumarin + NPG \rightarrow (Keto\text{-}coumarin\text{-}H)^{\bullet} + NPG_{(-H)}{}^{\bullet} \quad (r5)$$

$$NPG_{(-H)}{}^{\bullet} \rightarrow NPG_{(-H;-CO2)}{}^{\bullet} + CO_2 \quad (r6)$$

$$NPG_{(-H;-CO2)}{}^{\bullet} + Ar_2I^{+} \rightarrow NPG_{(-H;-CO2)}{}^{+} + Ar^{\bullet} + ArI \quad (r7)$$

$$(Keto\text{-}coumarin\text{-}H)^{\bullet} + Ar_2I^{+} \rightarrow Keto\text{-}coumarin + H^{+} + Ar^{\bullet} + ArI \quad (r8)$$

SCHEME 5 Proposed chemical mechanisms for photoinitiated polymerization using KC compounds[25,26] [Color figure can be viewed at wileyonlinelibrary.com]

Color online, B&W in print

Otherwise, as in other previously studied dye/Iod salt/amine combinations,[28] we suggest that r7 and r8 can be responsible for the interactions that take place in the three-component systems. Consequently, $Ar^{\bullet}$, $NPG_{(-H;-CO2)}{}^{\bullet}$, and keto-coumarin$^{\bullet+}$ ($KC^{\bullet+}$), $NPG_{(-H;-CO2)}{}^{+}$ can be considered as the initiating species for the FRP and the CP, respectively.

4 | CONCLUSION

In summary, a new series of KC derivatives is synthesized and proposed as excellent near-UV and visible light PIs to initiate both the CP of epoxides and the FRP of acrylates upon violet and blue LEDs. Great extinction coefficients, suitable oxidation potentials, and highly favorable free energy changes for the electron transfer reaction make these compounds efficient. The high photoreactivity of the KCs allows their use in laser write or even 3D printing experiments. The new initiating systems based on KC scaffold were also used for the synthesis of thick glass fiber photocomposites. Future development of other high-performance PIs suitable for 3D printing and preparation of photocomposites is under progress and will be presented in forthcoming works.

ACKNOWLEDGMENTS

IS2M thanks the "Region Grand-Est" for the funding of the Project MIPPI-4D. The Lebanese group would like to thank "The Association of Specialization and Scientific Guidance" (Beirut, Lebanon) for funding and supporting this scientific work. Mrs Claudio Apollonio and Matteo Balletti are acknowledged for the synthesis of some coumarins used in this work. Cyanagen srl is fully acknowledged for PhD fellowship to G. Rodeghiero.

ORCID

Jacques Lalevée https://orcid.org/0000-0001-9297-0335

REFERENCES

[1] D. Huang, J. Sun, L. Ma, C. Zhang, J. Zhao, *Photochem. Photobiol. Sci.* **2013**, *12*, 872.
[2] D. P. Specht, P. A. Martic, S. Farid, *Tetrahedron* **1982**, *38*, 1203.
[3] R. Nazir, P. Danilevicius, A. I. Ciuciu, M. Chatzinikolaidou, D. Gray, L. Flamigni, M. Farsari, D. T. Gryko, *Chem. Mater.* **2014**, *26*, 3175.
[4] G. Niu, W. Liu, H. Xiao, H. Zhang, J. Chen, Q. Dai, J. Ge, J. Wu, P. Wang, *Chem. Asian J.* **2016**, *11*, 498.
[5] K. Ramamurthy, E. J. P. Malar, C. Selvaraju, *New J. Chem* **2019**, *43*, 9090.
[6] J. L. R. Williams, D. P. Specht, S. Farid, *Polym. Eng. Sci.* **1983**, *23*, 1022.
[7] H. Salmi, H. Tar, A. Ibrahim, C. Ley, X. Allonas, *Eur. Polym. J.* **2013**, *49*, 2275.
[8] J. Lalevée, L. Zadoina, X. Allonas, J. P. Fouassier, *J. Polym. Sci. A Polym. Chem.* **2007**, *45*, 2494.
[9] J. P. Fouassier, J. Lalevée, *Photoinitiators for Polymer Synthesis, Scope, Reactivity, and Efficiency*; Wiley-VCH Verlag: Weinheim, Germany, **2012**.
[10] J.P. Fouassier, Ed. Hanser, Munich; New York; Cincinnati, **1995**.
[11] J. P. Fouassier, Ed., *Research Signpost*: Trivandrum, **2006**.
[12] K. Dietliker, SITA Technology Ltd., Edinburgh and London, **2002**.
[13] R. Zhou, J. P. Malval, M. Jin, A. Spangenberg, H. Pan, D. Wan, F. Morlet-Savary, S. Knopf, *Chem.Commun.* **2019**, *55*, 6233.
[14] Z. Li, X. Zou, G. Zhu, X. Liu, R. Liu, *ACS Appl. Mater. Interfaces* **2018**, *10*, 16113.
[15] W. Qiu, P. Hu, J. Zhu, R. Liu, Z. Li, Z. Hu, Q. Chen, K. Dietliker, R. Liska, *ChemPhotoChem.* **2019**, *3*, 1090.
[16] C. Dietlin, S. Schweizer, P. Xiao, J. Zhang, F. Morlet-Savary, B. Graff, J.-P. Fouassier, J. Lalevée, *Polym. Chem.* **2015**, *6*, 3895.
[17] J. Lalevée, N. Blanchard, M.-A. Tehfe, F. Morlet-Savary, J. P. Fouassier, *Macromolecules* **2010**, *43*, 10191.
[18] J. Lalevée, N. Blanchard, M.-A. Tehfe, M. Peter, F. Morlet-Savary, D. Gigmes, J. P. Fouassier, *Polym. Chem.* **2011**, *2*, 1986.
[19] D. Rehm, A. Weller, *Isr. J. Chem.* **1970**, *8*, 259.
[20] M. Abdallah, H. Le, A. Hijazi, M. Schmitt, B. Graff, F. Dumur, T. T. Bui, F. Goubard, J. P. Fouassier, J. Lalevée, *Polym.* **2018**, *159*, 47.
[21] J. Zhang, F. Dumur, P. Xiao, B. Graff, D. Bardelang, D. Gigmes, J. P. Fouassier, J. Lalevée, *Macromolecules* **2015**, *48*, 2054.
[22] P. Xiao, F. Dumur, J. Zhang, J. P. Fouassier, D. Gigmes, J. Lalevée, *Macromolecules* **2014**, *47*, 3837.
[23] B. Zhang, C. Ge, J. Yao, Y. Liu, H. Xie, J. Fang, *J. Am. Chem. Soc.* **2015**, *137*, 757.
[24] F. G. Medina, J. G. Marrero, M. Macías-Alonso, M. C. González, I. Córdova-Guerrero, A. G. Teissier García, S. Osegueda-Robles, *Nat. Prod. Rep.* **2015**, *32*, 1472.
[25] M. Abdallah, A. Hijazi, B. Graff, J.-P. Fouassier, G. Rodeghiero, A. Gualandi, F. Dumur, P. G. Cozzi, J. Lalevée, *Polym. Chem.* **2019**, *10*, 872.
[26] N. Zivic, M. Bouzrati-Zerelli, A. Kermagoret, F. Dumur, J. P. Fouassier, D. Gigmes, J. Lalevée, *ChemCatChem* **2016**, *8*, 1617.
[27] J. Lalevée, J. P. Fouassier, *Dyes and Chromophores in Polymer Science*; Wiley-ISTE: London, **2016**.
[28] P. Garra, B. Graff, F. Morlet-Savary, C. Dietlin, J.-M. Becht, J. P. Fouassier, J. Lalevée, *Macromolecules* **2018**, *51*, 57.

SUPPORTING INFORMATION

Additional supporting information may be found online in the Supporting Information section at the end of this article.

How to cite this article: Abdallah M, Dumur F, Hijazi A, et al. Keto-coumarin scaffold for photoinitiators for 3D printing and photocomposites. *J Polym Sci*. 2020;1–15. https://doi.org/10.1002/pol.20190290

Graphical Abstract

The contents of this page will be used as part of the graphical abstract of html only.
It will not be published as part of main.

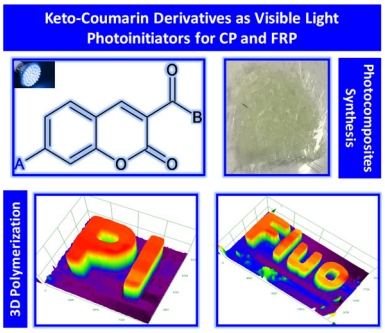

A new series of keto-coumarin derivatives is synthesized and proposed as excellent near-UV and visible light photoinitiators to initiate both the cationic polymerization of epoxides and the free-radical polymerization of acrylates upon violet and blue LEDs. The high photoreactivity of the KCs allows their use in laser write or even 3D printing experiments. The new initiating systems based on KC scaffold were also used for the synthesis of thick glass fiber photocomposites.